ELSEVIER

Inorganica Chimica Acta 242 (1996) 105–113

# Chiral ruthenium(IV)-oxo complexes. Structure, reactivities of $[Ru(terpy)(N\cap N)O]^{2+}$ ($N\cap N$ = *N*,*N*,*N*′,*N*′-tetramethyl-1,2-diaminocyclohexane) and $[Ru(Me_3tacn)(cbpy)O]^{2+}$ (cbpy = (−)-3,3′-[(4*S*-*trans*)-1,3-dioxolane-4,5-dimethyl]-2,2′-bipyridine)[1]

Wing-Chi Cheng[a], Wing-Yiu Yu[a], Jin Zhu[a], Kung-Kai Cheung[a], Shie-Ming Peng[b], Chung-Kwong Poon[a], Chi-Ming Che[a,*]

[a] *Department of Chemistry, The University of Hong Kong, Pokfulam Road, Hong Kong, Hong Kong*
[b] *Department of Chemistry, National Taiwan University, Taipei, Taiwan*

## Abstract

The complexes $[Ru^{IV}(terpy)(cxhn)O](ClO_4)_2$ (cxhn = *N*,*N*,*N*′,*N*′-tetramethyl-1,2-diaminocyclohexane, terpy = 2,2′:6′,2″(terpyridine) and $Ru^{IV}(Me_3tacn)(cbpy)O](ClO_4)_2$ (cbpy = (−)-3,3′-[(4*S*-*trans*)-1,3-dioxolane-4,5-dimethyl]-2,2′-bipyridine and $Me_3tacn$ = 1,4,7-trimethyl-1,4,7-triazacyclononane) have been prepared and crystal structures of $[Ru^{IV}(terpy)(cxhn)O](ClO_4)_2$ and $[Ru^{II}(Me_3tacn)(3,3'\text{-}Me_2bpy)(OH_2)](ClO_4)_2$ have been determined $[Ru^{IV}(terpy)(cxhn)O](ClO_4)_2$ $H_2O$, $C_{25}H_{35}Cl_2N_5O_{10}Ru$, $M_r = 737.68$, space group $P2_1/n$, monoclinic, $a = 8.215(5)$, $b = 14.650(7)$, $c = 24.261(10)$ Å, $\beta = 94\ 78(4)°$, $Z = 4$, $[Ru^{II}(Me_3tacn)(3,3'\text{-}Me_2bpy)(OH_2)](ClO_4)_2$, $C_{21}H_{35}Cl_2N_5O_9Ru$, $M_r = 673.52$, space group $P2_1/n$, monoclinic,. $a = 8.463(1)$, $b = 10.751(1)$, $c = 30.192(3)$ Å, $\beta = 91.77(1)°$, $Z = 4$. The Ru=O distance in $[Ru^{IV}(terpy)(cxhn)O](ClO_4)_2$ is 1.827(14) Å. All the ruthenium-oxo complexes react with alkenes to give the corresponding epoxides. Stoichiometric oxidation of styrene and 4-chlorostyrene by $[Ru^{IV}(terpy)(1R,2R\text{-}cxhn)O](ClO_4)_2$ gave the corresponding epoxide with no enantiomeric excess. Using $[Ru^{IV}(Me_3tacn)(cbpy)O](ClO_4)_2$, a 9% enantiomeric excess of *R*-styrene oxide and *R*-4-chlorostyrene oxide were found in the oxidation of both styrene and 4-chlorostyrene, respectively.

*Keywords:* Crystal structure; Ruthenium complexes; Oxo complexes; Chiral amine complexes

## 1. Introduction

The design of new oxidizing metal-oxo complexes has continued to be an important area of research [1]. Studies by various groups have revealed the rich oxidation chemistry of ruthenium-oxo complexes, which are active oxidants for organic oxidation [2]. Of particular interest to us is the oxoruthenium(IV) [3–5] because their reactions with alkenes are usually stereospecific and accompanied by a large and negative entropy of activation. Our desire to tackle asymmetric oxygen atom transfer reactions prompted us to study chiral ruthenium-oxo complexes with $C_2$ symmetric diamine ligand. Previously, we have prepared two different kinds of monooxoruthenium(IV) complexes, $[Ru^{IV}(terpy)(tmea)O]^{2+}$ [3a] (terpy = 2,2′:6′,2′(-terpyridine, tmea = *N*,*N*,*N*′,*N*′-tetramethyl-1,2-diaminoethane) and $[Ru^{IV}(Me_3tacn)(bpy)O]^{2+}$ [3c] ($Me_3tacn$ = 1,4,7-trimethyl-1,4,7- triazacyclononane, bpy = 2,2′-bipyridine), both of which are capable of oxidizing alkenes to epoxides. These two complexes adopt two different coordination geometries; the terpy-based complex has the Ru=O moiety nearly co-planar with chelating diamine while the $Me_3tacn$-based complex has the Ru=O moiety perpendicular to the coordinated 2,2′-bipyridine ligand. We would anticipate that introduction of the $C_2$ chiral diamine, *N*,*N*,*N*′,*N*′-tetramethyl-1,2-diaminocyclohexane (chxn), and chiral bipyridine (3,3′-[1,3-dioxolane-4,5-dimethyl-2,2′-bipyridine (cbpy) to the respective monooxoruthenium(IV) may afford enantiose-

---

* Corresponding author.

[1] Dedicated to Professor Harry B. Gray on the occasion of his 60th birthday.

*SSDI* 0020-1693(95)04855-2

lective alkene epoxidation. Herein is described the synthesis and reactivities of $[Ru^{IV}(terpy)(cxhn)O]^{2+}$ and $[Ru^{IV}(Me_3tacn)(cbpy)O]^{2+}$.

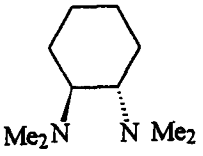

*1R, 2R*-**cxhn**

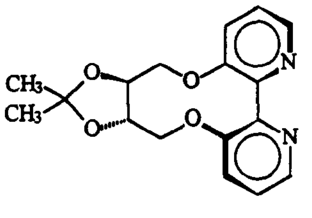

**(-)-cbpy**

## 2. Experimental section

### 2.1. Materials

$RuCl_3 \cdot 3H_2O$ (Johnson and Matthey) was used as received. Trifluoroacetic acid (99%, Aldrich) was purified by distillation under a nitrogen atmosphere. Silver trifluoromethanesulfonate (99+%, Aldrich) was dried in a vacuum oven. *rac*-1,2-Diaminocyclohexane (99%, mixture of *cis* and *trans*, Aldrich) was purified according to literature method to give the pure *trans*-compound before use. (–)-*1R,2R*-1,2-Diaminocyclohexane (98%, Aldrich) was used as received $Ru(terpy)Cl_3$, 3,3′-dimethyl-2,2′-bipyridine [6] (3,3′-$Me_2$bpy) and (–)-3,3′-[(4*S*-*trans*)-1,3-dioxolane-4,5-dimethyl-2,2′-bipyridine [7] (cbpy) were prepared according to published procedures.

#### 2.1.1. (–)-1R,2R-N,N,N′,N′-tetramethyl-1,2-diaminocyclohexane (1R,2R- cxhn)

The ligand was prepared by methylation of (–)-*1R,2R*-1,2-diaminocyclohexane (1 g) with a formic acid (10 ml)/formaldehyde (10 ml) mixture. The reaction mixture was refluxed for 48 h. After cooling to room temperature, it was neutralized with sodium hydroxide. The aqueous solution was extracted with chloroform (3 × 100 ml) and the combined organic layer was dried with anhydrous sodium sulfate.

The organic extract was evaporated to dryness to leave a viscous oil, which was vacuum distilled to afford a colorless liquid. Yield 90%. $[\alpha]_{589}^{22.3}$ –56.6° (c 0.603, MeOH).

#### 2.1.2. [Ru^II(terpy)(cxhn)(Cl)]ClO4 (1)

$Ru(terpy)Cl_3$ (0.2 g) was mixed with cxhn (0.2 g), lithium chloride (0.1 g), and triethylamine (5 drops) in aqueous ethanol (200 ml, 75% ethanol/25% water v/v). The reaction mixture gradually turned purple upon refluxing for 4 h. This was cooled to room temperature and filtered. The volume of the filtrate was reduced to ca. 15 ml. A saturated $NaClO_4$ solution was added to induce immediate precipitation of the product which was obtained as a purple solid, washed with water (10 ml), then with diethyl ether (50 ml), and air-dried. The product was recrystallized by diffusion of diethyl ether into an acetonitrile solution. Yield: 70%. *Anal.* Calc. for $C_{25}H_{33}Cl_2N_5O_4Ru$: C, 46.95; H, 5.16; N, 10.95. Found: C, 46.70; H, 5.04; N, 10.67%. UV-visible [in 0.1 M HCl, $\lambda_{max}$/nm ($\varepsilon_{max}$/$cm^{-1}$ $M^{-1}$)]: 561 (3310), 520 (3200), 380 (3480), 325 (18900), 283 (15400).

#### 2.1.3. [Ru^II(terpy)(cxhn)(H2O)](ClO4)2 (2)

A mixture of $[Ru^{II}(terpy)(cxhn)(Cl)]ClO_4$ (0.2 g) and silver trifluoromethanesulfonate (0.2 g) in 0.1 M $CF_3CO_2H$ (20 ml) was heated at 60°C for 30 min. The resulting deep purple solution was filtered to remove insoluble AgCl. To the filtrate $NaClO_4$ was added and the mixture was cooled in a refrigerator overnight. A dark microcrystalline solid gradually deposited and it was collected on frit. The complex was used without further purification. *Anal.* Calc. for $C_{25}H_{35}Cl_2N_5O_9Ru$: C, 41.60; H, 4.85; N, 9.71. Found: C, 41.19; H, 4.76; N, 9.25%. UV-visible [in 0.1 M $CF_3CO_2H$, $\lambda_{max}$/nm ($\varepsilon$/$cm^{-1}$ $M^{-1}$)]: 523 (2660), 460 (1870), 322 (26000),270 (17000).

#### 2.1.4. [Ru^IV(terpy)(cxhn)(O)](ClO4)2 (3)

$[Ru^{II}(terpy)(cxhn)(H_2O)](ClO_4)_2$ (0.1 g) was dissolved in a minimum amount of hot water. The resulting solution was filtered where necessary. The filtered solution was cooled in an ice-bath. Upon addition of an aqueous solution of $[NH_4]_2[Ce(NO_3)_6]$ (2 g in 5 ml), the color of the solution changed from purple to brown immediately. The product was obtained as a yellowish-brown microcrystalline solid upon addition of $NaClO_4$. *Anal.* Calc. for $C_{25}H_{33}Cl_2N_5O_9Ru$: C, 41.73; H, 4.62; N, 9.73. Found: C, 41.60; H, 4.70; N, 9.45%. UV-visible [in MeCN, $\lambda_{max}$/nm ($\varepsilon_{max}$/$cm^{-1}$ $M^{-1}$)] 352 (8000), 339 (9870), 278 (11000).

#### 2.1.5. [Ru^II(terpy)(1R, 2R-cxhn)Cl]ClO4

It was prepared by similar procedure as that of complex (1) except (–)-*1R,2R-N,N,N,N*-tetramethyl-1,2-diaminocyclohexane (1*R*,2*R*-cxhn) was used as the ligand. Its structure has been determined by X-ray crystal analysis [8].

#### 2.1.6. [Ru^IV(terpy)(1R, 2R-cxhn)O](ClO4)2

It was prepared by similar procedure as that of **3** using (–)-*1R,2R-N,N,N′,N′*-tetramethyl-1,2-diaminocyclohexane (1*R*,2*R*-cxhn) as the ligand.

#### 2.1.7. [Ru^II(Me3tacn)(3v32-Me2bpy)(OH2)](ClO4)2 (4)

A mixture of $Ru(Me_3tacn)Cl_3$ (50 mg), 3,3′-$Me_2$bpy (25 mg), and zinc metal powder (200 mg) in water (20 $cm^3$) was refluxed for 1 h. The reaction mixture gradually turned red. After cooling, the mixture was filtered to remove the zinc metal and unreacted ligand. A saturated $NaClO_4$ solution was added and the solution was left in a refrigerator overnight to afford dark red microcrystalline solid. The solid was collected on frit and washed with small amount of cold water. Yield: 64 mg (75%). *Anal.* Calc. for $C_{19}H_{29}N_5O_9Cl_2Ru$: C, 35.47; H, 4.54; N, 10.88. Found: C, 35.65; H, 4.60; N, 11.23%. UV-visible [in water, $\lambda_{max}$/nm ($\varepsilon_{max}$/dm$^3$ mol$^{-1}$ cm$^{-1}$)]: 238 (11620), 303 (19030), 358 (5310), 498 (3930) $^1$H NMR ($CD_3CN$): $\delta$ 9.07 (br s, 2H, H6 and H6′); 7.89 (d, 2H, H4 and H4′); 7.58 (br s, 2H, H5 and H5′) 3.31–2.75 (m, 21H, $Me_3$tacn); 2.36 (s, 6H, 2 × $CH_3$).

### 2.1.8. *$[Ru^{IV}(Me_3tacn)(3,3'\text{-}Me_2bpy)O](ClO_4)_2$(5)*

$[Ru^{II}(Me_3tacn)(3,3'\text{-}Me_2bpy)(OH_2)](ClO_4)_2$ (50 mg) was dissolved in deionized water (10 cm$^3$). The solution was cooled in an ice bath and an aqueous solution of $(NH_4)_2[Ce(NO_3)_6]$ (200 mg in 5 cm$^3$) was added. The solution changed immediately from deep red to light orange. A yellowish brown solid was precipitated upon addition of $NaClO_4$. Yield: 35 mg (70%). *Anal.* Calc. for $C_{19}H_{27}N_5O_9Cl_2Ru$: C, 35.57; H. 4.24; N. 10.91. Found: C, 35.52; H, 4.55; N, 10.42. Ultraviolet-visible [in water, $\lambda_{max}$/ nm ($\varepsilon_{max}$/dm$^3$ mol$^{-1}$ cm$^{-1}$)]: 315 (8900).

### 2.1.9. *$[Ru^{II}(Me_3tacn)(cbpy)Cl]PF_6$ (6)*

A mixture of $Ru^{III}(Me_3tacn)Cl_3$ (50 mg), cbpy (50 mg), and zinc metal powder (200 mg) in water (20 cm$^3$) was refluxed for 1 h. The reaction mixture gradually turned purple red. After cooling, the mixture was filtered to remove the zinc metal and unreacted ligand. A saturated $NH_4PF_6$ solution was added and purple precipitate immediately formed. The solid was collected on frit and washed with small amount of cold water. The product was then recrystallized from MeCN/$Et_2O$ mixture. Yield: 72 mg (70%). *Anal.* Calc. for $C_{26}H_{39}N_5O_4ClPF_6Ru$: C, 40.71; H, 5.08; N, 9.13. Found: C, 40.01; H, 4.88; N, 9.11%. Ultraviolet-visible [in water, $\lambda_{max}$/nm ($\varepsilon_{max}$/dm$^3$ mol$^{-1}$ cm$^{-1}$)]: 256 (8540), 329 (13000), 522 (2830).

### 2.1.10. *$[Ru^{II}(Me_3tacn)(cbpy)(OH_2)](PF_6)_2$ (7)*

A mixture of $[Ru^{II}(Me_3tacn)(cbpy)Cl]PF_6$ (0.1 g) and silver trifluoromethanesulfonate (0.2 g) in water (20 ml) was heated at 60°C for 30 min. The resulting deep red solution was filtered to remove insoluble AgCl. To the filtrate $NH_4PF_6$ was added, and the mixture was cooled in a refrigerator overnight. A red solid gradually deposited and it was collected on frit. The complex was used without further purification. Yield: 84 mg (70%). *Anal.* Calc. for $C_{26}H_{41}N_5O_5P_2F_{12}Ru$: C, 34.91; H, 4.58; N, 7.83. Found: C, 34.11; H, 4.43; N, 7.90%. Ultraviolet-visible [in water, $\lambda_{max}$/nm ($\varepsilon_{max}$/dm$^3$ mol$^{-1}$ cm$^{-1}$)]: 257(10130), 325 (11750), 511 (3000). $^1$H-NMR($CD_3CN$): 8.93 (dd, 1H, H6), 8.83 (dd, 1H, H6), 7.74 (ddd, 2H, H4, and H4), 7.64 (ddd, 2H, H5 and H5), 4.88–4.85 (m, 2H, –CH–CH,), 4.29–4.26 (m, 1H, –CH–$CH_2$), 4.20–4.15 (m, 3H, –CH–$CH_2$ and –CH–$CH_2$), 3.43–3.20 (m, 2H, $Me_3$tacn), 3.18–2.72 (m, 19H, $Me_3$tacn), 1.45 (s, 6H, 2 × –$CH_3$).

### 2.1.11. *$[Ru^{IV}(Me_3tacn)(cbpy)O](PF_6)_2$ (8)*

$[Ru^{IV}(Me_3tacn)(cbpy)O](PF_6)_2$ (0.1 g) was dissolved in a minimum amount of hot water. The resulting solution was filtered where necessary. The filtered solution was then cooled in an ice-bath, an aqueous solution of $[NH_4]_2[Ce(NO_3)_6]$ (2 g in 5 ml) was added, and the color of the solution changed from red to yellow immediately. The product was obtained as a yellowish-brown microcrystalline solid upon addition of $NH_4PF_6$. Yield: 75 mg (75%). *Anal.* Calc. for $C_{26}H_{39}N_5O_5P_2F_{12}Ru$: C, 34.90; H, 4.37; N, 7.85. Found: C, 34.75, H, 4.07; N, 7.85. Ultraviolet-visible [in water, $\lambda_{max}$/nm ($\varepsilon_{max}$/dm$^3$ mol$^{-1}$ cm$^{-1}$)]: 259 (9650), 356 (8650).

## 2.2. *Stoichiometric oxidation*

All stoichiometric reactions were carried out under an argon atmosphere using standard Schlenk techniques. In a typical run, hydrocarbon substrate (0.1 ml) in acetonitrile (2 ml) was degassed and filled with argon in a 10 ml Schlenk tube. This process was repeated for at least four times. $[Ru^{IV}(terpy)(cxhn)O](ClO_4)_2$ (**3**) or $[Ru^{IV}(Me_3tacn)(cbpy)O](ClO_4)_2$ (**8**) (30 mg) was added under a positive pressure of argon. The reaction mixture was stirred for 12 h. After addition of internal standard, the aliquot was taken for GLC or NE analysis for quantification. Gas chromatographic analyses were conducted by using a Hewlett-Packard 5890 series II with flame ionization detector and a HP-17 column (cross-linked 50% Ph Me Silicone, 0.2 $\mu$m film thickness). High purity grade nitrogen was used as the carrier gas. Component identification was established by comparing retention time with the authentic samples as well as gas chromatographic mass spectral analysis. Quantification of individual gas chromatographic components was performed by an internal standard method employing a Hewlett-Packard 3396 series II electronic integrator. The enantiomeric excess (e.e.) of styrene and 4-chlorostyrene oxide were determined by gas chromatographic technique using a chiral $\beta$-cyclodextrin column. The e.e. was found from the ratio of peak areas of the two enantiomers.

## 2.3. *Physical measurements and instrumentation*

UV-vis spectra were recorded on a Milton Roy (Spectronic 3000 Array) diode array spectrophotometer. IR spectra were obtained on a Nicolet model 20 FXT FT-IR spectrophotometer as Nujol mulls (4000–400 cm$^{-1}$). NMR spectra were run on a JEOL model FX 270 Q spectrometer. Cyclic voltammograms were recorded on a Princeton Applied Research Model 173 potentiostat and 175 universal programmer using an edge-plane pyrolytic graphite working electrode and a saturated calomel reference electrode (SCE).

## 2.4. *X-Ray structure analysis*

Crystal data: **3**·$H_2O$, $C_{25}H_{35}Cl_2N_5O_{10}Ru$, $M = 737.68$, space group $P2_1/n$, monoclinic, $a = 8.215(5)$,

Table 1

Atomic coordinates of non-hydrogen atoms of [Ru$^{IV}$(terpy)(cxhn)O](ClO$_4$)$_2$·H$_2$O

| | $x$ | $y$ | $z$ | $B_{iso}$[b] |
|---|---|---|---|---|
| Ru | 0.92237(25) | 0.68729(14) | 0.09667(8) | 2.80(9) |
| N1 | 0.7907(19) | 0.5629(11) | 0.0793(7) | 2.6(8) |
| N2 | 0.9047(18) | 0.6805(13) | 0.0133(7) | 3.2(9) |
| N3 | 1.0388(21) | 0.8085(14) | 0.0775(7) | 4.0(10) |
| N4 | 0.9329(19) | 0.6929(14) | 0.1868(6) | 3.3(9) |
| N5 | 0.6814(21) | 0.7622(12) | 0.1068(7) | 3.3(9) |
| O | 1.1161(17) | 0.6257(10) | 0.0987(6) | 3.8(8) |
| C1 | 0.730(3) | 0.5045(16) | 0.1131(9) | 3.6(12) |
| C2 | 0.664(3) | 0.4232(19) | 0.0963(10) | 4.4(14) |
| C3 | 0.656(3) | 0.3958(17) | 0.0412(10) | 4.1(12) |
| C4 | 0.716(3) | 0.4547(16) | 0.0057(9) | 3.7(12) |
| C5 | 0.185(3) | 0.5389(16) | 0.0250(9) | 3.4(12) |
| C6 | 0.841(3) | 0.6091(15) | −0.0115(9) | 3.1(11) |
| C7 | 0.831(3) | 0.6030(17) | −0.0688(9) | 3.9(12) |
| C8 | 0.888(3) | 0.6748(23) | −0.0983(10) | 6.1(17) |
| C9 | 0.9663(24) | 0.7512(18) | −0.0705(9) | 3.9(13) |
| C10 | 0.9785(24) | 0.7535(16) | −0.0122(10) | 3.4(12) |
| C11 | 1.0449(24) | 0.8234(16) | 0.0212(8) | 3.3(11) |
| C12 | 1.139(3) | 0.8971(18) | 0.0018(10) | 4.4(13) |
| C13 | 1.212(3) | 0.9606(18) | 0.0368(11) | 5.5(15) |
| C14 | 1.189(3) | 0.9483(18) | 0.0909(10) | 4.5(13) |
| C15 | 1.100(3) | 0.8752(16) | 0.1090(10) | 3.9(12) |
| C16[a] | 0.805(4) | 0.7614(24) | 0.2028(13) | 0.7(7) |
| C16′[a] | 0.772(5) | 0.707(3) | 0.2025(17) | 3.0(10) |
| C17 | 0.776(3) | 0.7490(16) | 0.2645(9) | 3.7(5) |
| C18[a] | 0.659(6) | 0.833(4) | 0.2787(20) | 4.9(13) |
| C18′[a] | 0.605(6) | 0.757(3) | 0.2776(19) | 4.0(11) |
| C19 | 0.517(4) | 0.8307(24) | 0.2466(14) | 8.8(9) |
| C20 | 0.530(3) | 0.8207(19) | 0.1850(10) | 5.0(6) |
| C21′[a] | 0.650(5) | 0.745(3) | 0.1636(17) | 2.6(9) |
| C21[a] | 0.711(4) | 0.7913(21) | 0.1678(12) | 0.3(7) |
| C22 | 0.950(5) | 0.5944(19) | 0.2104(12) | 8.4(22) |
| C23 | 1.083(3) | 0.7335(21) | 0.21-15(10) | 5.7(15) |
| C24 | 0.542(3) | 0.7112(21) | 0.0785(11) | 6.8(17) |
| C25 | 0.6908(25) | 0.8520(18) | 0.0802(10) | 4.7(14) |
| Cl1 | 0.4116(9) | 0.4942(6) | 0.2233(3) | 6.2(4) |
| O1 | 0.364(4) | 0.4117(21) | 0.1955(12) | 15.5(23) |
| O2 | 0.410(3) | 0.5699(19) | 0.1875(11) | 12.8(18) |
| O3 | 0.576(3) | 0.4832(21) | 0.2407(11) | 13.3(20) |
| O4 | 0.319(3) | 0.5061(21) | 0.2689(10) | 12.5(19) |
| Cl2 | 0.4982(9) | 0.8488(5) | 0.9045(3) | 5.9(4) |
| O5 | 0.583(4) | 0.816(3) | 0.9477(10) | 18.4(28) |
| O6 | 0.356(3) | 0.7929(16) | 0.8969(10) | 10.4(16) |
| O7[a] | 0.448(5) | 0.933(3) | 0.8803(18) | 8.7(26) |
| O7′[a] | 0.464(4) | 0.937(3) | 0.9376(19) | 8.6(28) |
| O8[a] | 0.597(5) | 0.789(4) | 0.8689(21) | 13.5(39) |
| O8′[a] | 0.576(5) | 0.868(3) | 0.8594(15) | 8.7(26) |
| O9 | 0.886(3) | 0.0547(20) | 0.1406(11) | 12.5(19) |

[a] Atoms with occupancy = 0.5.

[b] $B_{iso}$ is the mean of the principal axes of the thermal ellipsoid.

$b = 14.650(7)$, $c = 24.261(10)$ Å, $\beta = 94.78(4)°$, $U = 2910(4)$ Å$^3$, $D_c = 1.684$ g cm$^{-3}$, $Z = 4$, $F(000) = 1512$, $\mu$(MoK$\alpha$) = 7.7 cm$^{-1}$.

A crystal dimension of 0.15 × 0.30 × 0.30 mm of **3**·H$_2$O was used for data collection at 21°C on a Nonius diffractometer (graphite monochromatized MoK$\alpha$ radiation), $\lambda = 0.7107$ Å using $\theta$–$2\theta$ scan mode technique ($2\theta_{max} = 45°$) at National Taiwan University. A total of 3790 unique reflections were obtained, 1639 of which were considered ($|F_o2| \geq 2.0\sigma|F_o|$) observed and used in structure refinement. Data reduction and structure refinement were performed using the NRCVAX program. The final least square refinement was calculated with 368 variables and was reached at $R_f = 0.087$, $R_w = 0.079$, and $S = 2.40$ with weights based on counting statistics. The final difference map showed residual extrema in the range −0.830 to +0.940 e Å$^{-3}$.

**4**: $C_{21}H_{35}Cl_2N_5O_9Ru$, $M = 673.52$, space group $P2_1/n$, monoclinic, $a = 8.463(1)$, $b = 10.751(1)$, $c = 30.192(3)$ Å, $\beta = 91.77(1)°$, $U = 2745.7(8)$ Å$^3$, $D_c = 1.634$ mg m$^{-3}$, $Z = 4$, $F(000) = 1384$, $\mu$(MoK$\alpha$) = 8.1 cm$^{-1}$.

A crystal dimension of 0.15 × 0.1 × 0.25 mm of **4** was used for data collection at 24°C on a Nonius diffractometer (graphite monochromatized MoK$\alpha$ radiation, $\lambda = 0.71073$ Å using $\theta$–$2\theta$ scan mode technique ($2\theta_{max} = 46°$) at The University of Hong Kong. Intensity data ($2\theta_{max} = 46°$; $h$ 0–9, $k$ 0–11, $l$ −33–33) were collected for Lorentz and polarization effects. A total of 4036 independent reflections were obtained of which 2433 reflections with $I > 3.0\sigma(I)$ were considered observed and used in the structural analysis. The structure was solved by Patterson and Fourier methods and subsequent refinement by full matrix least squares using the Enraf-Nonius SPD-1985 Programs on a MicroVAX II computer The 38 non-H atoms were refined anisotropically. The 2 hydrogen atoms of the water molecules were located in the difference Fourier synthesis and the positional parameters were refined. All the other H atoms at calculated positions with isotropic thermal parameters equal to 1.3 times that of the attached C atoms were not refined. Convergence for 349 variables by least squares refinement of $F$ with $w = 4F_o^2/\sigma^2(F_o^2)$, where $\sigma^2(F_o^2) = [\sigma^2(I) + (0.040F_o^2)^2]$ was reached at $R = 0.039$ and $R_w = 0.049$ and $S = 1\ 28$. $(\Delta/\sigma)_{max} = 0\ 01$ for atoms of the complex cation. The final difference Fourier map was featureless, with maximum positive and negative peaks of 0.42 and 0.36 e Å$^{-3}$ respectively.

Tables 1 and 2 list the atomic coordinates of non-hydrogen atoms for complexes **3** and **4**, respectively. Select-ed bond distances and angles are given in Tables 3 and 4.

## 3. Results and discussion

### 3.1. Syntheses and characterization

Although the use of chiral $N,N,N',N'$-tetramethyl-1,2-diaminocyclohexane in asymmetric alkene dihydroxylation is well documented [9], there has been no report on the details concerning the preparation and purification of this ligand. In this work, it was prepared by methylation of the chiral 1,2-diaminocyclohexane with a HCHO/HCOOH mixture The optical purity of chiral (−)-(1$R$,2$R$)-

Table 2

Atomic coordinates of non-hydrogen atoms of [Ru$^{\mathrm{II}}$(Me$_3$tacn)(3,3′-Me$_2$bpy)(OH$_2$)][ClO$_4$]$_2$

| Atom | *x* | *y* | *z* | *B*(A2) |
|---|---|---|---|---|
| Ru | 0.31226(6) | 0.06629(5) | 0.13131(2) | 2.475(9) |
| Cl1 | 0.8749(2) | 0.0650(2) | 0.29553(6) | 4.32(4) |
| Cl2 | 0.1358(2) | 0.1836(2) | −0.03613(6) | 3.60(4) |
| O | 0.1239(5) | 0.0722(5) | 0.0804(2) | 4.1(1) |
| O11 | 0.8044(7) | −0.0315(5) | 0.2696(2) | 6.5(1) |
| O12 | 0.7674(8) | 0.1111(7) | 0.3248(2) | 10.2(2} |
| O13 | 0.9273(7) | 0.1620(6) | 0.2673(2) | 6.6(2) |
| O14 | 1.0128(9) | 0.0211(9) | 0.3182(3) | 10.5(3) |
| O21 | −0.0149(7) | 0.1920(7) | −0.0187(2) | 8.3(2) |
| O22 | 0.1381(7) | 0.0913(6) | −0.0699(2) | 6.4(2) |
| O23 | 0.2456(7) | 0.1515(9) | −0.0028(2) | 3.8(2) |
| O24 | 0.179(1) | 0.2962(6) | −0.0551(3) | 9.3(2) |
| N1 | 0.1829(6) | −0.0396(5) | 0.1790(2) | 3.1(1) |
| N2 | 0.4902(6) | 0.0535(6) | 0.1801(2) | 3.6(1) |
| N3 | 0.3873(6) | −-0.1162(5) | 0.1135(2) | 3.6(1) |
| N4 | 0.4482(6) | 0.1718(5) | 0.0890(2) | 2.7(1) |
| N5 | 0.2280(6) | 0.2493(5) | 0.1430(2) | 3.0(1) |
| C1 | 0.0081(8) | −0.0204(8) | 0.1776(3) | 4.4(2) |
| C2 | 0.5691(9) | 0.1750(9) | 0.1907(3) | 5.3(2) |
| C3 | 0.402(1) | −0.1388(7) | 0.0653(3) | 5.0(2) |
| C4 | 0.2503(9) | 0.0033(9) | 0.2227(2) | 4.4(2) |
| C5 | 0.4276(9) | −0.0009(9) | 0.2226(2) | 4.9(2) |
| C6 | 0.6114(8) | −0.0343(8) | 0.1622(3) | 4.8(2] |
| C7 | 0.5361(8) | −0.1443(8) | 0.1395(3) | 4.9(2) |
| C8 | 0.2565(9) | −0.2033(8) | 0.1282(3) | 4.9(2) |
| C9 | 0.2136(9) | −0.1754(8) | 0.1744(3) | 4.9(2) |
| C10 | 0.5821(8) | 0.1363(7) | 0.0700(2) | 3.6(2) |
| C11 | 0.6835(5) | 0.2167(8) | 0.0503(3) | 4.4(2) |
| C12 | 0.6489(9) | 0.3414(8) | 0.0511(3) | 4.6(2) |
| C13 | 0.5136(9) | 0.3841(7) | 0.0696(2) | 3.6(2) |
| C14 | 0.4071(8) | 0.2950(6) | 0.0861(2) | 2.4(1) |
| C15 | 0.2581(8) | 0.3244(6) | 0.1084(2) | 3.0(1) |
| C16 | 0.1491(9) | 0.4157(6) | 0.0942(2) | 3.8(2) |
| C17 | 0.0283(9) | 0.4447(8) | 0.1232(3) | 5.1(2) |
| C18 | 0.0146(9) | 0.3840(8) | 0.1622(3) | 4.9(2) |
| C19 | 0.1127(8) | 0.2823(7) | 0.1707(2) | 3.9(2) |
| C20 | 0.492(1) | 0.5223(7) | 0.0739(3) | 5.6(2) |
| C21 | 0.145(1) | 0.4735(8) | 0.0483(3) | 5.4(2) |

Table 3a

Selected bond distances (Å) of [Ru$^{\mathrm{IV}}$(terpy)(cxhn)(O)](ClO$_4$)$_2$ (3)

| | |
|---|---|
| Ru–O | 1.827(14) |
| Ru–N(l) | 2.143(16) |
| Ru–N(2) | 2.017(17) |
| Ru–N(3) | 2.088(20) |
| Ru–N(4) | 2.184(15) |
| Ru–N(5) | 2.294(14) |

Table 3b

Selected bond angles (°) of [Ru$^{\mathrm{IV}}$(terpy)(cxhn)(O)](ClO$_4$)$_2$ (3)

| | | | |
|---|---|---|---|
| O–RU–N(1) | 90.6(7) | N(1)–Ru–N(5) | 90.1(7) |
| O–Ru–N(2) | 89.6(7) | N(2)–Ru–N(3) | 79.3(7) |
| O–Ru–N(3) | 90.7(7) | N(2)–Ru–N(4) | 178.0(6) |
| O–Ru–N(4) | 91.7(7) | N(2)–Ru–N(5) | 98.1(6) |
| O–RU–N(5) | 172.2(6) | N(3)–Ru–N(4) | 102.2(7) |
| N(l)–Ru–N(2) | 76.6(7) | N(3)–Ru–N(5) | 91.9(7) |
| N(l)–Ru–N(3) | 155.8(7) | N(4)–Ru–N(5) | 80.6(6) |
| N(l)-Ru-N(4) | 101.9(7) | | |

*N*,*N*,*N*′,*N*′-tetramethyl-1,2-diaminocyclohexane was found to be greater than 95% e.e. by chiral GC analysis. Previous studies showed that the [Ru$^{\mathrm{II}}$(terpy)(tmea)(Cl)]$^{2+}$ complex, where tmea = *N*,*N*,*N*′,*N*′-tetramethyl-1,2-diaminoethane, could be prepared by refluxing Ru(terpy)Cl$_3$ with the chelating diamine in ethylene glycol [3a,3b]. However for the reaction of Ru(terpy)Cl$_3$ with cxhn in ethylene glycol under refluxing condition, the ruthenium product was found to be [Ru$^{\mathrm{II}}$(terpy)$_2$]$^{2+}$. Changing the solvent from ethylene glycol to aqueous ethanol does lead to the successful synthesis of [Ru$^{\mathrm{II}}$(terpy)(cxhn)Cl](ClO$_4$)$_2$ (**1**).

Various research groups have reported the introduction of chiral appendages at the 4,4′-, 5,5′- and 6,6′- positions of 2,2′-bipyridines. These chiral bipyridine ligands have been used in organic syntheses with satisfactory asymmetric induction [10]. However, there are not many examples of having incorporation of $C_2$ symmetry chiral auxiliary at the 3,3′-position. In fact, 3,3′-disubstituted 2,2′-bipyridines suffer from labile atropisomerism [7]. With 3,3′-Me$_2$bpy, the [Ru$^{\mathrm{II}}$(Me$_3$tacn)(3,3′-Me$_2$bpy)(OH$_2$)](ClO$_4$)$_2$ complex **4** was prepared using similar procedure as reported for [Ru$^{\mathrm{II}}$(Me$_3$tacn)(bpy)(OH$_2$)](ClO$_4$)$_2$ [3c]. Unfortunately, resolution of the two diastereoisomers of **4** was futile. To tackle this problem, we employed the chiral (−)-3,3′-[(4*S*-*trans*)-1,3-dioxolane-4,5-dimethyl-2,2′-bipyridine (cbpy) ligand, which was reported by Lucchi and co-workers [7]. The chirality of this ligand is fixed by a side chain derived from optically active tartaric

Table 4a

Selected bond distances (Å) of [Ru$^{\mathrm{II}}$(Me$_3$tacn)(3,3′-Me$_2$bpy)(OH$_2$)](ClO$_4$)$_2$ (3)

| | |
|---|---|
| Ru–O | 2.176(4) |
| Ru–N(1) | 2.158(5) |
| Ru–N(2) | 2.075(5) |
| Ru–N(3) | 2.136(6) |
| Ru–N(4) | 2.079(5) |
| Ru–N(5) | 2.125(5) |

Table 4b

Selected bond angles (°) of [Ru$^{\mathrm{II}}$(Me$_3$tacn)(3,3′-Me$_2$bpy)(O)](ClO$_4$)$_2$ (3)

| | | | |
|---|---|---|---|
| O–Ru–N(l) | 96.5(2) | N(2)–Ru–N(3) | 84.5(2) |
| O–Ru–N(2) | 177.8(2) | N(2)–Ru–N(4) | 94.1(3) |
| O–Ru–N(3) | 93.7(3) | N(2)–Ru–N(5) | 100.5(2) |
| O–Ru–N(4) | 87.5(2) | N(3)–Ru–N(4) | 100.0(2) |
| O–Ru–N(5) | 81.3(2) | N(3)–Ru–N(5) | 174.7(2) |
| N(l)–Ru–N(2) | 82.0(3) | N(4)–Ru–N(5) | 78.0(3) |
| N(l)–Ru–N(3) | 81.0(2) | N(4)–C(14)–C(15) | 113 2(6) |
| N(l)–Ru–N(4) | 176.0(2) | N(4)–C(15)–C(14) | 114.0(5) |
| N(l)–Ru–N(5) | 101.5(3) | | |

Table 5
UV-visible spectral data of the ruthenium complexes

| Complex | Solvent | $\lambda_{max}$/nm ($\varepsilon_{max}$/cm$^{-1}$ M$^{-1}$) |
|---|---|---|
| $[Ru^{II}(terpy)(cxhn)(Cl)]ClO_4$ | 0.1 MHCl | 561(3310), 520(3200) 380(3480), 325(18900) 283(15400) |
| $[Ru^{II}(terpy)(cxhn)(H_2O)](ClO_4)_2$ | 0.1 M $CF_3CO_2H$ | 523(2660), 460(1870) 322(26000), 270(17000) |
| $[Ru^{IV}(terpy)(cxhn)(O)](ClO_4)_2$ | MeCN | 352(8000), 339(9870) 278(11000) |
| $[Ru^{II}(Me_3tacn)(3,3'Me_2\text{-}bpy)(OH_2)](ClO_4)_2$ | $H_2O$ | 238(11620), 303(19030) 358(5310), 498(3930) |
| $[Ru^{II}(Me_3tacn)(3,3'Me_2\text{-}bpy)(O)](PF_6)_2$ | MeCN | 315(8900) |
| $[Ru^{II}(Me_3tacn)(cbpy)(Cl)](PF_6)$ | MeOH | 256(8540), 329(13000) 522(2830) |
| $[Ru^{II}(Me_3tacn)(cbpy)(OH_2)](PF_6)_2$ | $H_2O$ | 257(10130), 325(11750), 511(3000) |
| $[Ru^{IV}(Me_3tacn)(cbpy)(O)](PF_6)_2$ | MeCN | 259(9650), 356(8650) |

acid. The crystal structure of $[Pt(cbpy)Cl_2]$ has been determined [11]. Reaction of $Me_3tacnCl_3$ with 1 equiv. of cbpy in the presence of zinc metal and in water afforded complex **6** quantitatively.

Complexes **2** and **7** were prepared by reacting Ag(I) with the parent chloro-complexes in aqueous media. They were then oxidized by $[NH_4]_2[Ce(NO_4)_6]$ in water to give the corresponding oxoruthenium(IV) complexes All the newly prepared ruthenium-oxo complexes are stable for months if stored at −30°C. In highly purified acetonitrile, however, they are stable for hours at room temperature but would be reduced to $Ru^{II}$ upon prolonged standing. The UV-visible spectral data are summarized in Table 5. As expected, all the aqua complexes show low energy $d_\pi(Ru) \rightarrow p_\pi$, *(terpy/bpy) absorption in the visible region. As with other $Ru^{IV}$=O complexes, the UV-visible absorption spectra of **3**, **5**, **8** are featureless in the visible region. These $Ru^{IV}$=O complexes have similar IR spectra as that of the parent aqua-complexes indicating that the ligand remains intact throughout the synthesis. The $\nu$(Ru=O) for **3**, **5**, **8** are at 775, 783, 796 cm$^{-1}$ respectively. Similar $\nu$(Ru=O) stretching frequencies have previously been reported.

In all cases, the aqua complexes display similar electrochemistry as that of the corresponding monooxoruthenium(IV). Cyclic voltammograms of **2**, **4** and **7** in pH 1.1 (0.1 M $CF_3CO_2H$) with edge-plane pyrolytic electrode as working electrode are shown in Fig. 1a–c. All these complexes display a reversible $Ru^{III/II}$ and a quasi-reversible $Ru^{IV/III}$ couple. At pH 1.1, the $E°[Ru^{IV/III}]$ for **2** and **7** are equal to 0.90 V versus SCE, whereas it is equal to 0.86 V versus SCE for **4**. On the other hand, the $Ru^{III/II}$ couple for **2** is found to be 0.75 V versus SCE which is 220 mV and 160 mV more anodic than that for **4** and **7**, respectively. As expected, these $E°$ values change cathodically for approximately 60 mV for each unit of pH change. This is consistent with one electron, one proton

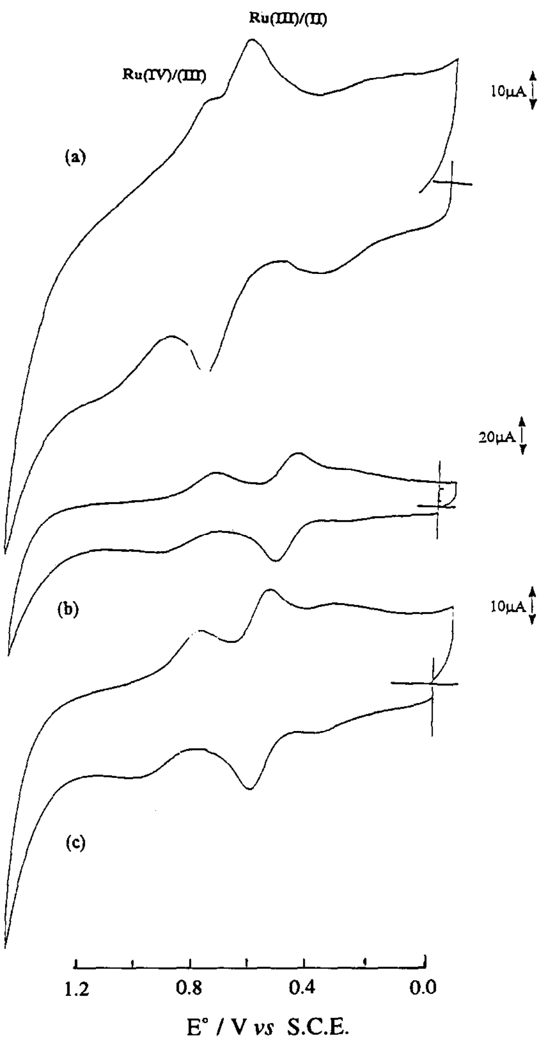

Fig. 1. Cyclic voltammogram of (a) $[Ru^{II}(terpy)(cxhn)(OH_2)](ClO_4)_2$, (b) $[Ru^{II}(Me_3tacn)(3,3'\text{-}Me_2bpy)(H_2O)](ClO_4)_2$ and (c) $[Ru^{II}\text{-}(Me_3tacn)(cbpy)(OH_2)](ClO_4)_2$ [in 0.1 M $CF_3CO_2H$. Scan rate, 100 mV s$^{-1}$; working electrode, edge-plane pyrolytic graphite.

transfer based on the Nernstian prediction of −59 mV per pH unit (Scheme 1).

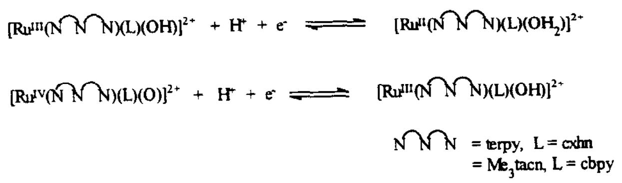

Scheme 1.

### 3.2. X-Ray structural determinations of 3 and 4

Fig. 2 shows a perspective view of the $[Ru^{IV}(terpy)(cxhn)(O)]^{2+}$ cation. The cxhn ligand is in racemate form. The coordination around the ruthenium is distorted octahedral with the terpy ligand in a meridional configuration. The cyclohexyl ring of the cxhn ligand is disordered. The Ru=O distance is 1.827(14) Å, which is shorter than that of 1.862(8) Å found in $[Ru^{IV}(py)_4(O)]^{2+}$ [12] but longer than that of 1.765(5) Å in the monooxo-ruthenium(IV) complexes with macrocyclic tertiary amines [13]. The X-ray structure of $[Ru^{II}(terpy)(1R,2R\text{-}cxhn)Cl]ClO_4$ has been determined by X-ray crystal analysis [8]. This complex crystallizes in a space group of $P2_1$ [8].

Since satisfactory crystals of **6**–**8** suitable for X-ray crystal analysis have not been obtained, the crystal structure of $[Ru^{II}(Me_3tacn)(3,3'\text{-}Me_2bpy)(OH_2)]^{2+}$, which could be a model for probing the spatial arrangement of the coordinated 3,3′-disubstituted-2,2′-bipyridine ligand around the Ru–$Me_3$tacn moiety, has been determined. Fig. 3 shows a perspective view of the complex cation of **4**. The complex has a distorted octahedral geometry with $Me_3$tacn facially coordinated to Ru. The measured Ru–$OH_2$ distance of 2.176(4) Å is comparable to that of 2.168(3) Å in $[Ru^{II}(Me_3tacn)(bpy)(OH_2)]^{2+}$ [3c] and 2.151(17) Å in $[Ru^{II}(terpy)(tmea)(OH_2)]^{2+}$ [14]. As expected, the 3,3′$Me_2$bpy is not planar due to transannular steric interaction of the two methyl groups. The dihedral angle is 54.2(4)°. This dihedral angle is significantly larger than that of 37.4° between the two isoquinoline rings of BIQN in $[Ru^{II}(terpy)(BIQN)Cl]^+$ [15] (where BIQN = 1,1′-biisoquinoline). The X-ray structure of $Pt(cbpy)Cl_2$ showed that the chirality of cbpy remains intact upon coordination and the dihedral angle between the two pyridine rings of cbpy is 37.7° [11].

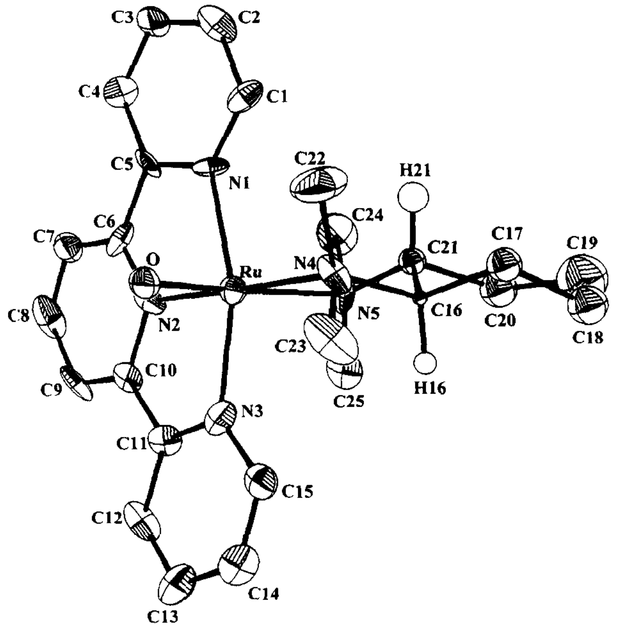

Fig. 2. A perspective view of the complex $[Ru^{IV}(terpy)(cxhn)O]^{2+}$ cation.

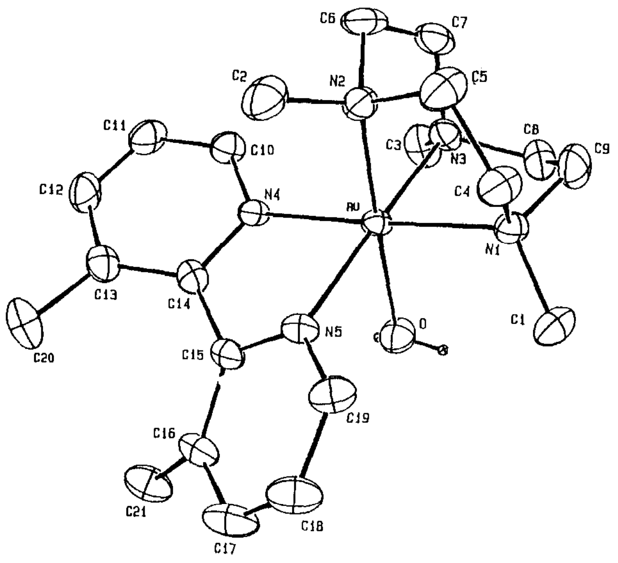

Fig. 3. A perspective view of the complex $[Ru^{II}(Me_3tacn)(3,3'\text{-}Me_2bpy)(H_2O)]^{2+}$ cation.

### 3.3. Stoichiometric oxidation of alkenes

Previous studies [3] showed that monooxoruthenium(IV) complexes containing chelating tertiary diamine and diimine ligands could oxidize alkenes under mild conditions. Similarly, **3** and **8** are competent oxidants. Table 6 summarizes the results of stoichiometric oxidation in acetonitrile at room temperature. The ruthenium products after the oxidation are $[Ru^{II}(terpy)(cxhn)(MeCN)]^{2+}$ and $[Ru^{II}(Me_3tacn)(cbpy)(MeCN)]^{2+}$, which have their MLCT absorptions at 480 and 460 nm, respectively.

Oxidation of styrene gave styrene oxide predominantly and a minor amount of benzaldehyde. With *cis*-stilbene, the major product was *cis*-stilbene oxide (94%) although some *trans*-stilbene oxide (6%) was also detected. On the other hand, oxidation of *trans*-stilbene afforded *trans*-stilbene oxide exclusively.

The results of epoxidation of styrene and 4-chlorostyrene by the chiral $[Ru^{IV}(terpy)(1R,2R\text{-}cxhn)(O)]^{2+}$ and

Table 6

Results of stoichiometric oxidation of alkenes by $[\mathrm{Ru^{IV}(terpy)(cxhn)(O)}]^{2+}$ (**3**) and $[\mathrm{Ru^{IV}(Me_3tacn)(cbpy)(O)}]^{2+}$ (**8**) in acetonitrile at 298 K

| Substrates | Products[a] | Yield (%)[b] | |
|---|---|---|---|
| | | 3 | 8 |
| Styrene | Styrene oxide | 68 | 56 |
| | Benzaldehyde | 14 | 10 |
| 4-Chlorostyrene | 4-Chlorostyrene oxide | 60 | 58 |
| | | 15 | 12 |
| Norbornene | *exo*-2,3-Epoxynorbornane | | 92 |
| *cis*-Cyclooctene | *cis*-Cyclooctene oxide | 18.6 | |
| Cyclohexene | Cyclohexene oxide | 8.3 | |
| | Cyclohex-2-ene-1-ol | 21.5 | |
| | Cyclohex-2-ene-1-one | 67.1 | |
| *trans*-Stilbene | *trans*-Stilbene oxide[c] | 48 | |
| *cis*-Stilbene | *cis*-Stilbene oxide[c] | | |
| | *trans*-Stilbene oxide[c] | | |

[a] Products were identified and subsequently quantified by gas chromatography.

[b] Product yield is based on the amount of ruthenium oxidant used.

[c] Products were identified and subsequently quantified by $^1$H NMR using *m*-toluic acid as internal standard.

$[\mathrm{Ru^{IV}(Me_3tacn)(cbpy)O}]^{2+}$ complexes are summarized in Table 7. Enantiomeric excess (e.e.) was determined by $^1$H NMR spectroscopy in the presence of the chiral shift reagent (–)-Eu(hfc)$_3$ and/or using chiral GC analysis. *R*-form styrene oxide was obtained but with rather low enantiomeric excess (<10% e.e.). This is in contrast to the results reported by Jacobsen [16], Groves [17] and others [18] for asymmetric catalytic oxidation of styrene using chiral manganese Schiff base and iron porphyrin complexes.

## 4. General comment

The results of stoichiometric oxidation and kinetic studies show that oxidation of alkenes by **3** give organic epoxides with minor rearranged products. The observed large and negative $\Delta S^‡$ values [19] suggested association of the Ru=O moiety and C=C bond in the rate-limiting step. However, no asymmetric induction was found for the epoxidation of styrene by $[\mathrm{Ru^{IV}(terpy)}(1R,2R\text{-}\mathrm{cxhn})(\mathrm{O})]^{2+}$. These could be rationalized by examining the possible directions of approach of alkene to the $\mathrm{Ru^{IV}{=}O}$ moiety as described in Fig. 4. In this figure, the full structure of the ligands and the methyl groups are not shown for lucidity. Presumably, the alkene would approach the $\mathrm{Ru^{IV}{=}O}$ on the side with the C=C molecular plane perpendicular to the equatorial plane defined by terpyridine. This direction of approach would assume a maximum orbital interaction between the $\pi$-bonding orbital of alkene and the Ru–O$\pi^*$ orbital.

Table 7

Stoichiometric oxidation of alkenes by $[\mathrm{Ru^{IV}(terpy)(cxhn)(O)}]^{2+}$ (**3**) and $[\mathrm{Ru^{IV}(Me_3tacn)(cbpy)(O)}]^{2+}$ (**8**) in acetonitrile at 298 K

| Substrate | Products | Enantiomeric excess[b] (e.e.%) | |
|---|---|---|---|
| | | 3 | 8 |
| Styrene | Styrene oxide | 0 | 9[a] |
| 4-Chlorostyrene | 4-Chlorostyrene oxide | 0 | 9[a] |

[a] (*R*)-epoxide is the major product.

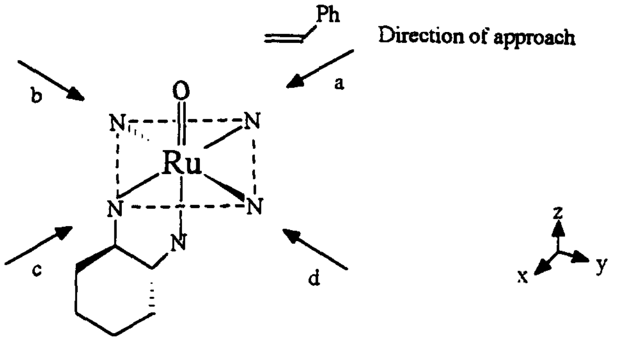

Fig. 4. Possible directions of approach of alkeline molecule to $\mathrm{Ru^{IV}{=}O}$ moiety.

Established by crystal analysis of complex **3**, the chiral cxhn ligand is colinear with the axis defined by the $\mathrm{Ru^{IV}{=}O}$ moiety and is orthogonal to the terpyridine ligand. Although the cyclohexyl ring is disorder in solid state, a chair conformation is presumably much favored in solution. Direction (a) is the most unhindered one but both prochiral faces of styrene can move towards the $\mathrm{Ru^{IV}{=}O}$ moiety without interacting with the chiral diamine ligand. The fact that the $\Delta S^‡$ values for the oxidation of styrene and norbornene by $[\mathrm{Ru^{IV}(terpy)(L{\frown}L)O}]^{2+}$ (L⌒L = chelating diamine or diimine ligands) are quite insensitive to the structure of L⌒L suggests very little interaction of alkene and L⌒L in the rate-limiting step [19]. Opposite to direction (a) is (c) where the approach of alkene is blocked by the bulky methyl groups situated in the course of the trajectory.

However, directions (b) and (d) are not unhindered, but the prochiral face differentiation arising from the approach along (d) would be canceled out by that brought about along direction (b). As a result, no enantiomeric excess of epoxide was obtained.

In contrast to the merdional geometry of terpy, the Me$_3$tacn ligand coordinates to ruthenium in a facial configuration. Its steric bulkiness is expected to guard against free approach of alkene molecule (Fig. 5).

From the crystal structure of $[\mathrm{Ru^{IV}(Me_3tacn)(bpy)O}]^{2+}$, the Ru=O moiety is virtually perpendicular to the bipyridine ligand and is hidden inside the bulky Me$_3$tacn. Thus it is reasonable to find that introduction of chiral appendages on the bipyridine ligand could lead to enantioselec-

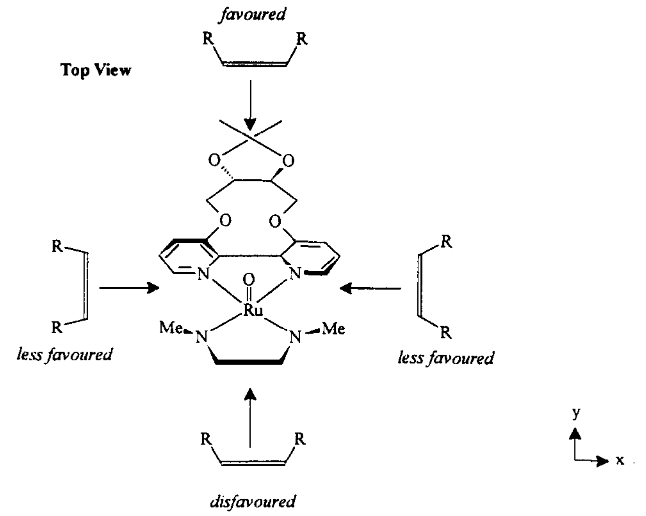

Fig. 5.

tive alkene epoxidation. Indeed, oxidation of both styrene and 4-chlorostyrene by $[\mathrm{Ru^{IV}(Me_3tacn)(cbpy)O}]^{2+}$ afforded a 9% enantiomeric excess of the *R*-styrene oxide and *R*-4-chlorostyrene oxide respectively (Table 7), although the asymmetric induction is not impressive when compared with other reported works [16–18]. Since the proximity of the reaction site to the chirality of the ligand is an important factor governing the stereochemical course of oxidation, the low enantiomeric excess could be attributed to the chirality on the cbpy ligand, which is too remote from the Ru=O moiety. However, recent studies showed that a chiral ruthenium-oxo complex bearing a $C_2$ symmetric chiral tridentate imine, $[\mathrm{Ru^{IV}(2,6\text{-}pz^*2py)(bpy)O}]^{2+}$, (2,6-pz*2py = 2,6-bis[(4*S*,7*R*)-7,8,8-indazolyl]pyridine; bpy = 2,2-bipyridine), is able to mediate asymmetric epoxidation of unfunctionalized alkenes with reasonable e.e. [20]. Jacobsen and others recently reported that the chiral and sterically bulky manganese Schiff base complexes are effective catalysts for asymmetric epoxidation of a variety of alkenes [21]. In their studies, a chiral $\mathrm{Mn^V}$ oxo species, which has not been characterized, was proposed to be the active intermediate [22]. Of particular interest is the structural similarity between the proposed $\mathrm{Mn^V{=}O}$ intermediate and complex **8**.

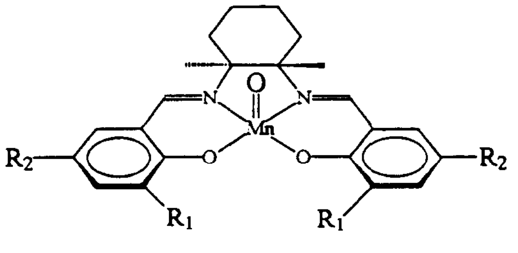

Mn(V)-oxo

## Acknowledgements

We acknowledge the financial support from The University of Hong Kong and The Hong Kong Research Council.

## References

[1] (a) W.A. Nugent and J.M. Mayer, *Metal-Ligand Multiple Bonds,* Wiley, New York, 1988; (b) R.H. Holm, *Chem Rev, 87* (1987) 1401; (c) R.A. Sheldon and J.K. Kochi, *Metal-Catalysed Oxidation of Organic Compounds;* Academic Press, New York, 1981.

[2] (a) W.P. Griffith, *Chem. Soc. Rev., 21* (1992) 179; (b) C.M. Che and V.W.W. Yam,. *Adv. Inorg Chem, 39* (1992) 233; (c) C.M. Che, *Pure and Appl. Chem., 67* (1995) 225.

[3] (a) C. Ho, T.C. Lau and C.M. Che, *J. Chem. Soc., Dalton Trans.,* (1990) 967; (b) C.M. Che, C. Ho and T.C. Lau, *J. Chem. Soc., Dalton Trans.,* (1991) 1901. (c) W.C. Cheng, W.Y. Yu, K.K. Cheung and C.M. Che, *J. Chem. Soc., Dalton Trans.,* (1994) 57.

[4] (a) J.C. Dobson, W.K. Seok and T.J. Meyer, *Inorg. Chem., 25* (1986) 1513; (b) L.K. Stultz, R.A. Binstead, M.S. Reynolds and T.J. Meyer, *J. Am. Chem. Soc., 117* (1995) 2520.

[5] (a) M.E. Marmion and K.J. Takeuchi, *J. Chem. Soc., Daltons Trans.,* (1988) 2385. (b) M.E. Marmion, R.A. Leising and K.J. Takeuchi, *J. Coord. Chem., 19* (1988) 1.

[6] M. Tiecco, L. Testaferri, M. Tingoli, D. Chianelli and M. Montanucci, *Synthesis, 8* (1984) 736.

[7] C. Botteghi, A. Schionato and O.D. Lucchi, *Synth. Commun., 21* (1991) 1819.

[8] S.M. Peng and C.M. Che, unpublished results.

[9] M. Tokles and J.K. Snyder, *Tetrahedron Lett., 27* (1986) 3951.

[10] See for examples: (a) S. Gladiali., L. Pinna, G. Delogu, S.D. Martin, G. Zassinovich and G. Mestroni, *Tetrahedron Asym, 1* (1990) 635; (b) S. Gladiali, L. Pinna, G. Delogu, E. Graf and H. Brunner, *Tetrahedron Asym., 1* (1990) 937. (c) C. Bolm and M. Ewald, *Tetrahedron Lett, 31* (1990) 5011. (d) C. Bolm, G. Schlingloff and K. Harms, *Chem. Ber, 125* (1992) 1191. (e) C. Bolm, M. Ewald and M. Felder, *Chem. Ber., 125* (1992) 1205.

[11] K.K. Cheung and C.M. Che, unpublished results.

[12] K. Aoyagi, Y. Yukawa, K. Shimizu, M. Mukaida, T. Takeuchi and H. Kakihana, *Bull. Chem. Soc. Jpn., 59* (1986) 1493.

[13] C.M. Che, K.Y. Wong and T.C.W. Mak, *J. Chem. Soc., Chem. Commun.,* (1985) 546.

[14] N. Grover, N. Gupta, P. Singh and H.H. Thorp, *Inorg Chem., 31* (1992) 2014.

[15] W.Y. Yu, W.C. Cheng, C.M. Che and Y. Wang, *Polyhedron,* 13 (1994) 2963.

[16] W. Zhang, J.L. Loebach, S.R. Wilson and E.N. Jacobsen, *J. Am. Chem. Soc., 112* (1990) 2801.

[17] J.T. Groves and R.S. Myers, *J. Am. Chem. Soc., 105* (1983) 5791.

[18] D. Mansuy, P. Battoni, J.-P. Renaud and P. Guerin, *J. Chem. Soc., Chem. Commun.,* (1985) 155.

[19] W.Y. Yu, *Ph.D. Thesis,* The University of Hong Kong (1993).

[20] W.H. Fung, W.C. Cheng, W.Y. Yu, C.M. Che and T.C.W. Mak, *J. Chem. Soc., Chem. Commun.,* (1995) 2007.

[21] E.N. Jacobsen, W. Zhang and M.L. Güller, *J. Am. Chem. Soc., 113* (1991) 6703.

[22] (a) E.N. Jacobsen, W. Zhang, A.R. Muci, J.R. Ecker and L. Deng, *J. Am. Chem. Soc., 113* (1991) 7063; (b) B.D. Brandes and E.N. Jacobsen, *J. Org. Chem., 59* (1994) 4378; (c) S. Chang, J.M. Galvin and E.N. Jacobsen, *J. Am. Chem. Soc., 116* (1994) 6937; (d) M. Palucki, P.J. Pospisil, W. Zhang and E.N Jacobsen, *J. Am. Chem. Soc., 116* (1994) 9333.